Bursty Fluctuation Characteristics in SOL/Divertor Plasmas of Large Helical Device

N. Ohno1), S. Masuzaki2), V. P. Budaev3), H. Miyoshi4), S. Takamura4), T. Morisaki2), N. Ohyabu2), A. Komori2)

1) EcoTopia Science Institute, Nagoya Univ., Nagoya, Aichi-ken 464-8601, Japan
2) National Institute for Fusion Science, Toki, Gifu-ken 506-5292, Japan
3) Nuclear Fusion Institute, RCC Kurchatov Institute, 123182, Kurchatov, Moscow, Russia
4) Graduate School of Engineering, Nagoya Univ. Nagoya, Aichi-ken 464-8603, Japan

e-mail: ohno@ees.nagoya-u.ac.jp

Abstract. Bursty electrostatic fluctuation in the scrape off layer (SOL) and the divertor region of the Large Helical Device (LHD) have been investigated by using a Langmuir probe array on a divertor plate and a reciprocating Langmuir probe. Large positive bursty events were often observed in the ion saturation current measured with a divertor probe near the divertor leg at which the magnetic line of force connected to the area of a low-field side with a short connection length. Condition averaging result of the positive bursty events indicates the intermittent feature with a rapid increase and a slow decay is similar to that of plasma blobs observed in tokamaks. On the other hand, at a striking point with a long connection length, negative spikes were observed. Statistical analysis based on probability distribution function (PDF) was employed to investigate the bursty fluctuation property. The observed scaling exponents disagree with the predictions for the self-organized criticality (SOC) paradigm.

1. Introduction

From experiments on fusion devices, there are a lot of evidence that plasma turbulence is highly intermittent[1-6]. Intermittent events play a crucial role in transport dynamics. Intermittent transport resulted from rare, large events is accompanied by coherent structures, leading to heat and particle losses more than ones predicted by classical diffusive scaling. The cross-field transport in the scrape-off layer (SOL), associated with the intermittent events, determines the heat and particle deposition width on a divertor target plate and a first wall. Moreover, the prediction of the peak value of the intermittent heat deposition on plasma-facing components becomes important because the lifetime of the plasma-facing components is determined by not only the averaged heat load but also the peak value of the intermittent one.

Probabilistic approach to plasma turbulence and transport allows one to consider most important questions in the prediction of transport, including non-locality of transport in the edge plasma turbulence. Fluctuation properties observed in the edge region of magnetized plasmas were found to be similar, suggesting the universality of self-similarity properties[4]. In tokamaks, intermittent convective plasma transport, so-called "plasma blob" has been one of the most important issues, which produces flatter density profile (2^{nd} SOL) in the SOL of tokamaks[7]. Electrostatic bursty fluctuation of ion saturation currents (I_{sat}) and/or floating potentials measured with Langmuir probes are analyzed to obtain fundamental properties of the plasma blobs[8,9].

On the other hand, in helical devices, there are few systematic studies on the SOL's fluctuation property focusing on the intermittent bursty fluctuation. Recently, a fast camera observation showed the radial motion of filaments in the edge of the Large Helical Device (LHD)[10], suggesting the convective cross-field transport. Detailed comparison of the

intermittent bursty fluctuation properties in the edge plasmas of tokamak and helical fusion devices is expected to give an essential understanding of the blobby plasma transport, because the blobby plasma transport is thought to be strongly influenced by the magnetic configuration. In this paper, intermittent bursty fluctuation properties in the edge of the LHD have been investigated by analyzing the I_{sat} measured with a probe array embedded in an outboard divertor plate and a reciprocating probe. Statistical analysis based on probability distribution function (PDF)[11] is employed to investigate the intermittent evens in the electrostatic fluctuation.

2. Magnetic Structure of LHD and Experimental Setup

The LHD has a set of $l = 2/ m = 10$ continuous helical coil and three sets of poloidal coils, producing heliotron-type magnetic configuration[10]. The major radius R is 3.9 m and the averaged minor radius a is 0.65 m. Fig. 1(a) shows typical magnetic structure of horizontally elongated cross-section at a magnetic axis position $R_{rm} = 3.53$ m. The edge magnetic structure is so complicated than that in the SOL of divertor tokamaks. An intrinsic divertor exists without additional coils, and four plasma legs reach the divertor plates. This magnetic configuration is so-called natural helical divertor. Ion particle flux to the divertor plates follows the deposition profile of the magnetic field lines.

Ion saturation current I_{sat} was measured with a Langmuir probe array (16 electrodes) embedded in an outer divertor plate as shown in Fig. 1(b). The probe electrode was dome-type with a diameter of 1 mm, made of graphite. The interval between the probe electrodes is 6 mm. The probe electrodes are numbered from 1 to 16 staring from the lower right of Fig. 2(b). The lower numbered probes are located in a low field side and higher numbered ones in a high field side, because the magnetic field strength near the helical coils is always strong as shown by the contour of equi-magnetic field strength in Fig. 1(a). The profile of the I_{sat} in the open field line layers was also measured by a reciprocating Langmuir probe shown in Fig. 1(c).

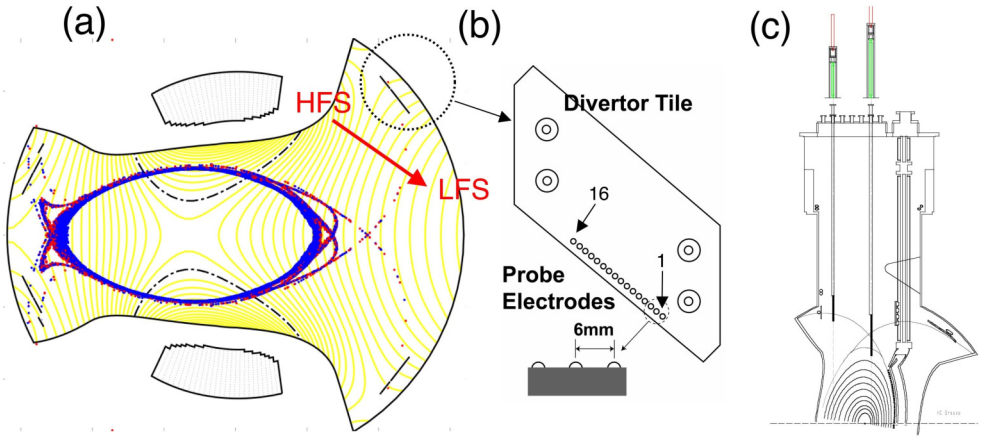

FIG. 1 (a) Schematics of LHD magnetic configuration in horizontally elongated cross section for the magnetic axis of R_{rm} =3.53 m, (b) Scheme of the Langmuir probe configuration on the divertor plate, (c) Configuration of the reciprocating Langmuir probe.

3. Fluctuation Properties at the Divertor of the LHD

3.1 Fourier and wavelet analysis

Fig. 2(a) shows the profiles of connection length L_c of magnetic lines of force, starting from

the outboard divertor plate tile having the probe array and averaged I_{sat} measured with the divertor probe array in a hydrogen discharge at B = 2.5 T, R_{ax} = 3.53 m and $\bar{n}_e$ = 1.5x10^{19} m^{-3}. L_c varies from less than a few meters to over a few kilometers. The field line with large L_c reaches the ergodic layer surrounding the core plasma region. Then, the probe, which is connected to the field line with large L_c, has large ion particle flux like probe 10.

Figs. 2(b)-(d) show the time evolution of I_{sat} at probe 9, 10 and 11. The sampling time is 4 μs. The time traces look like quite different fluctuation property. A lot of intermittent positive spikes were clearly observed at probe 9 as shown in Fig. 2(b). On the other hand, the negative spikes appear in the I_{sat} of probe 10. In Fig. 2(d), the time evolution of I_{sat} at the probe 11 has no intermittent bursts although there is relatively large averaged I_{sat}.

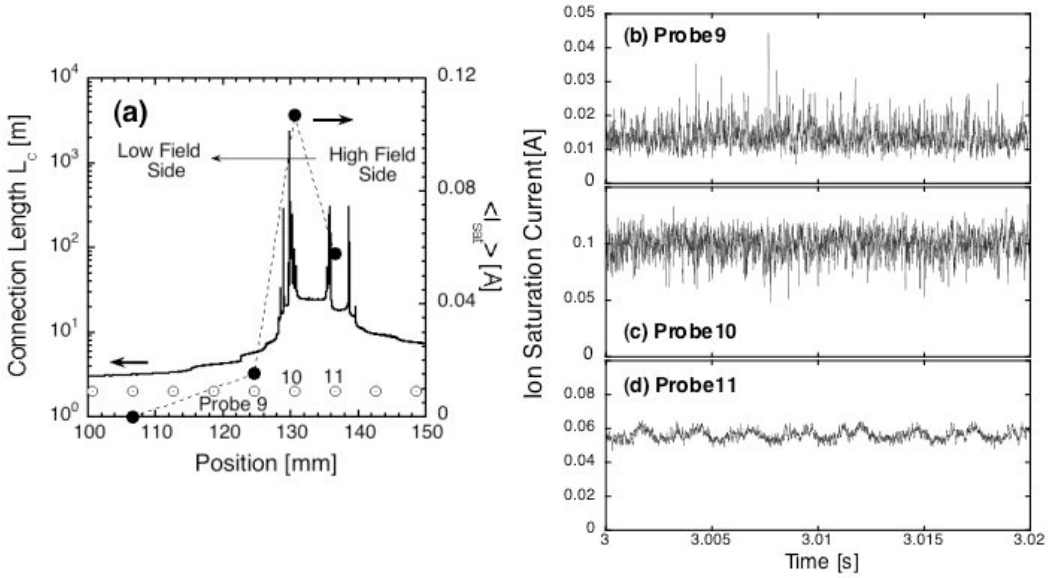

FIG. 2 (a) Distribution of field connection length L_c at a magnetic axis R_{ax} of 3.53 m. Open circles show the positions of the probe electrodes. Averaged I_{sat} measured with the probes are shown as closed circles. Time evolution of ion saturation currents I_{sat} at different probe positions: (b) 9, (c) 10 and (d) 11 in Fig. 2(a).

The scaling features of the fluctuation can be studied by mean of Fourier analysis. Figs. 3(a)-(c) show the spectral density, corresponding to Figs. 2(b)-(d) respectively. All figures have no peaks in $S(f)$, indicating no periodic fluctuation in the I_{sat}. In high b discharges, periodic fluctuation was sometimes detected in I_{sat}. The fluctuation frequency matches that of MHD fluctuations in the core plasma region, detected by magnetic probes. This phenomenon is quite interesting in term of core-edge plasma coupling, such as propagation of the fluctuation from core to edge region through the ergodic region. However, this phenomenon is beyond the scope in this article. We will focus on the electrostatic intermittent fluctuations.

The shapes of the spectral density $S(f)$ allow one to conclude whether the scaling behavior of a time series can be described by power-law dependences of the type $S(f) = f^{-\alpha}$. The power spectrum of the turbulent fluctuations quantifies the properties of the process. In fluid mechanics, Kolmogorov theory predicts the inertial sub-range, having a power law dependence, $S(f) = f^{-1}$. A self-organized criticality (SOC) model was proposed to analyze non-local plasma transport in tokamaks[12]. In the SOC model, the emitted avalanche leads to convection in contrast to the diffusive transport. The SOC model predicts a power law

dependence, $S(f) = f^{-1}$. In recent tokamak experiment[13], avalanchelike phenomena in electron temperature fluctuation were observed, whose characteristics were associated with the SOC model. In our experiments, several scaling ranges with respect to the frequency are registered in the frequency spectra of the fluctuation, with no f^{-1} behavior as shown in Fig. 3. Similar behavior of power spectra was obtained in other experiments using Langmuir probes in edge plasmas. The typical value of the scaling exponent of the power spectra in the high frequency is in the range of a ≈ -2.

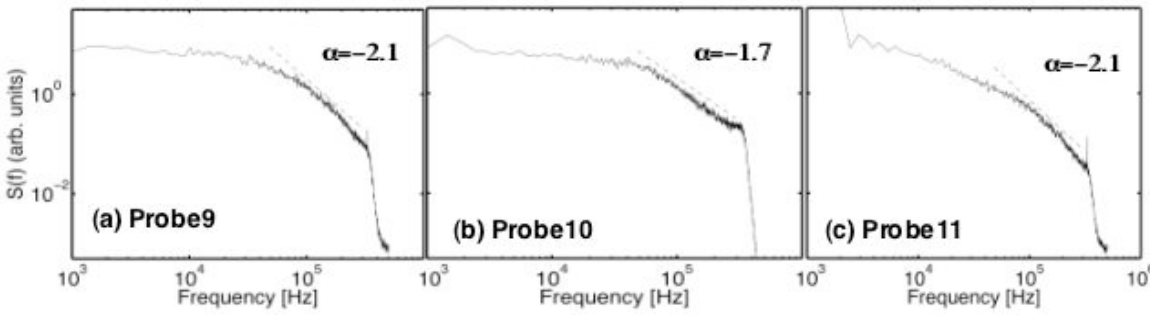

FIG. 3 Power spectra $S(f) = |I_{sat}(f)|^2$ of the I_{sat} measured at different probe positions: (a) 9, (b) 10 and (c) 11 in Fig. 2(a). The power law fitting by $S(f) = f^{-\alpha}$ are shown by dashed-dot lines.

In general, Fourier analysis is unsuitable for analysis of the time trace data including intermittent events. Alternative method is wavelet decomposition process, which can catch the characteristics of intermittent events. The I_{sat} in Figs. 2(b) and (c) were analyzed with a complex Morlet wavelet decomposition, shown in Fig. 4. Although Fourier analysis of the I_{sat} gives no apparent peaks in the frequency domain, the strong intensities (red regions) of the wavelet decomposition appear at a wavelet scale between 40 and 100 μs, which means that the pulse signals with a time width between 40 and 100 μs are dominating. Both wavelet decomposition patterns are quit similar, which would indicate a relation between them.

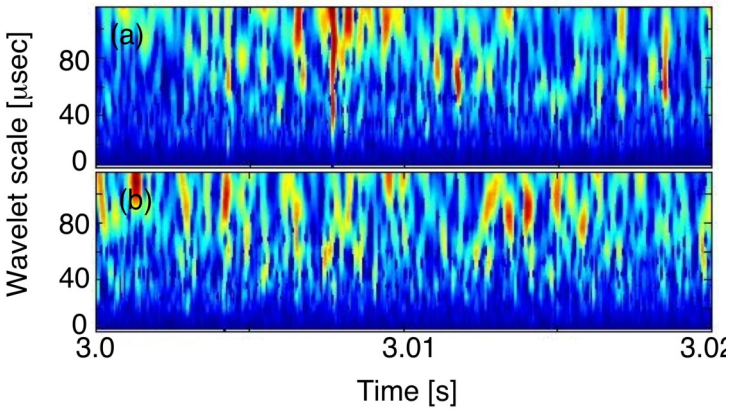

FIG. 4 Wavelet decomposition with complex Morlet wavelet for I_{sat} corresponding to Fig. 2(b) and (c).

3.2 Statistical analysis based on probability distribution function (PDF)

Conventional method like Fourier analysis gives few fluctuation properties in signals with intermittent events. The detailed feature of the fluctuation can be in investigated by a probabilistic analysis. We have analyzed fluctuation property of I_{sat} based on probability distribution function (PDF). The PDF is an important statistical quantity for turbulence research. In order to obtain PDF, we construct a histogram of the time evolution of I_{sat}. Fig. 5 shows PDFs corresponding to Figs. 2(b)-(d). For fully random signal, a PDF has a Gaussian profile shown by dashed lines in Fig. 5. The PDF (open circles) of the I_{sat} at probe 9 is

non-Gaussian profile and positively skewed, meaning that large positive bursts are much greater than expected value from a fully random distribution. On the other hand, the PDF of I_{sat} at probe 10 is negatively skewed. The PDF for probe 11 matches a Gaussian profile. Deviation of PDF from a Gaussian profile can be quantitatively characterized by skewness $S=\langle x^3\rangle/\langle x^2\rangle^{3/2}$ and flatness $F=\langle x^4\rangle/\langle x^2\rangle^2$. In the Gaussian distribution, S and F are 3 and 0, respectively. Large skewness of 1.23 and flatness of 6.46 were obtained in Fig.2 (b). Although the probe 10 is only 6 mm depart away from the probe 9, the I_{sat} shows many negative spikes and the sign of S changes to negative (-0.42).

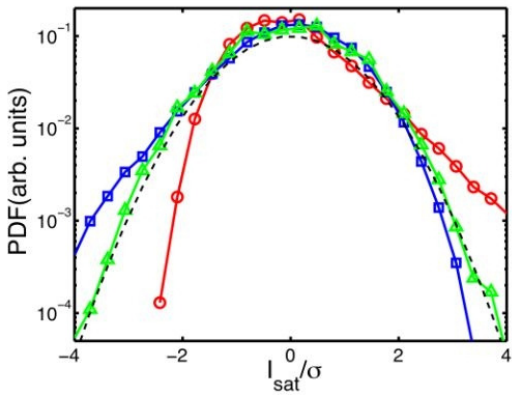

FIG. 5 Log-linear plots of probability distribution function (PDF) for I_{sat} at probe 9 (circles), 10 (squares), 11 (triangles). Dashed line show a Gaussian profile

In order to investigate characteristic timescales of the fluctuation of I_{sat}, we define $\delta I = I_{sat}(t) - I_{sat}(t-\tau)$, where τ is delayed time. When a time trace would obey a Poisson process having fully random process, the PDF of δI becomes a Gaussian profile for any τ. Fig. 6(a) shows the PDFs of δI, corresponding to the I_{sat} in Fig. 2(b), by varying τ from 4 μs to 1024 μs. As increasing τ, the PDF is getting closer to a Gaussian distribution. Skeweness of the δI's PDF is plotted as a function of τ in Fig. 6(b). For small τ, the value of skewness is positive. At τ is larger than τ_c =100 μs, the skewness becomes almost zero, indicating that the PDF is changed to a Gaussian profile. The time τ_c corresponds an integral correlation time scale of the fluctuation, and can be interpreted as an inertial-range timescale discussed in fluid dynamics. Fig. 6(c) also shows the skewness of δI's PDF, corresponding to I_{sat} in Fig. 2(c) as a function of τ. Although the skewness changes from negative value to zero, the time scale τ_c is almost same as that in Fig. 6(b). These could suggest that some instability, producing positive and negative density spikes, occurs between the field lines connected to the probe 9 and 10 from the divertor plate to X point.

The SOC model has been widely used to explain fluctuation properties including avalanche process driven by gradients and resilience of plasma profiles as mentioned before. On the other hand, the discrepancy between experimental results and SOC model prediction was also reported in the reversed field pinch (RFP) device by using waiting-time statistics [14]. The LHD is very suitable device for testing the SOC paradigm because the LHD have very long plasma discharge, which can give an advantage for

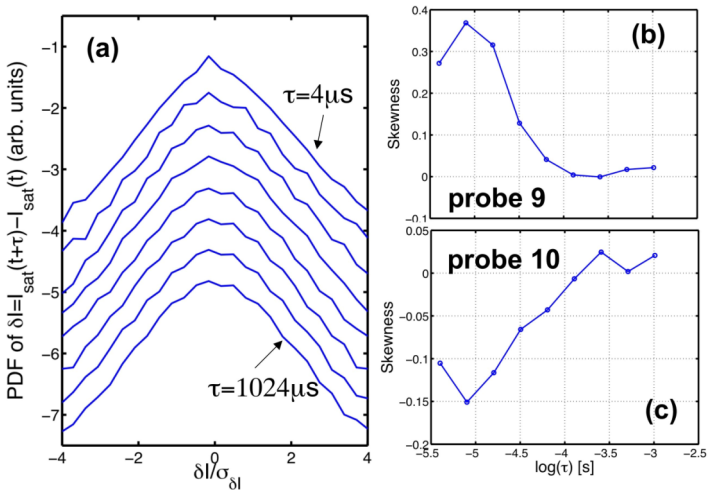

FIG. 6 (a) Log-linear plots of probability distribution function (PDF) for $\delta I = I_{sat}(t) - I_{sat}(t-\tau)$ as a parameter of delayed time τ, corresponding to the I_{sat} in Fig. 2(b). Skewness of δI's PDF as a function of τ for the I_{sat} (b): in Fig. 2(b) and (c): in Fig. 2(c).

probabilistic analysis**.** We have analyzed waiting-time statistics of I_{is} with positive burst events in Fig. 2(b). The SOC model predicts that the PDF of the waiting times τ_d between successive burst evens should be an exponential law: $P(\tau_d) \propto \exp(-\tau_d)$. The definition of τ_d is shown in Fig. 7(a) where the burst events are determined by spikes with amplitude above twice of the standard deviation of the original signal (horizontal solid line). Fig. 7(b) shows the PDF for the waiting times reconstructed by a statistical ensemble for 250000 data points obtained during the period of the discharge with constant plasma parameters. Logarithmic plot of Fig. 7(b) gives the power factor of the PDF scaling to be -2.8, which is quite different from the SOC prediction. Thus, the waiting time statistic of I_{is} at divertor probes in the LHD is in contrast with the prediction of the SOC model, which is consistent with the power law of the power spectrum mentioned before. These experimental results are similar ones observed in the RFP plasma.

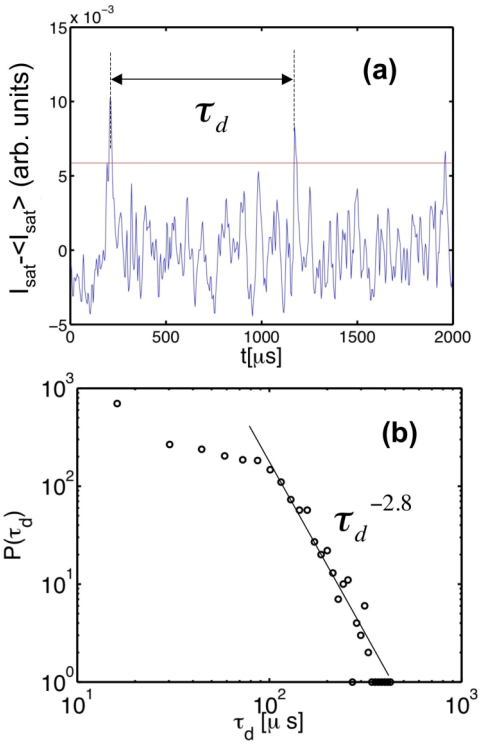

FIG. 7 (a) Definition of time interval (waiting time) τ_d between subsequent intermittent bursts, (b) probability density of the waiting time τ_d. Power law fit is shown by the solid line.

4. Discussion

4.1 Blobby plasma transport in the LHD

In low field sides of SOL in tokamaks, positive bursts, associated with radial propagation of plasma blobs, have been observed in I_{sat} by the Langmuir probe measurements. Theory predicts that plasma blobs propagate toward a low field side due to ***E***x***B*** drift, where the electric field ***E*** in the plasma blob is generated by the poloidal charge separation due to gradient ***B*** drift. In the LHD, magnetic field strength is large near the helical coils. Direction of gradient ***B*** is shown in Fig. 1(a). Then, probe 9 is located at a low field side from the divertor leg, where positive bursts are observed. On the other hand, at probe 10 located at high field side, there is no positive burst. This tendency is consistent with the theoretical prediction for plasma blobs.

In order to reveal the typical burst's profile, conditional averaging method was employed. In this method, large bursts with a peak above four times as large as the standard deviation of the original signal are selected and averaged in the same time domain. The result of the I_{sat} averaged over 480 events indicates that the positive spikes have the common property of a rapid increase and slow decay shown in Fig. 8. This feature is similar to that of plasma blobs in tokamaks.

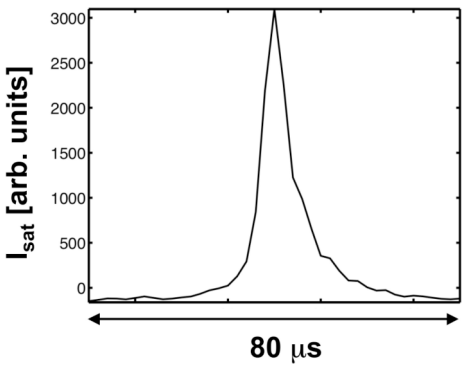

FIG. 8 Conditional averaging result of the I_{sat} of Fig. 2 (b).

To investigate the fluctuation property near divertor legs in an open field line layer, the profile

of I_{sat} was measured by the reciprocating Langmuir probe shown in Fig. 1(c). Fig 9 (a) shows the profile of I_{sat} across a divertor leg, in which two peaks were observed around Z = 1.35 m and Z = 1.38 m, where Z is a distance from the equatorial plane of the LHD. The locations of the peaks are corresponding to the regions with large connection length L_c. As shown in Fig. 9(b), between the two I_{sat}'s peaks, the values of skewness is almost zero or slightly negative. On the other hand, at Z more than 1.38 m corresponding to the low field side of the divertor leg, the skewness as well as the fluctuation amplitude increases with Z. This result is consistent with the observation at the divertor probe array mentioned above, which suggests the possibility of the blobby plasma transport in the LHD. The inset of Fig. 9(b) shows the logarithmic plot of the I_{sat} above Z = 1.35 m. The I_{sat} decays exponentially. There is no flat profile (so called second SOL), which has been often observed in the far-SOL of tokamaks associated with blobby plasma transport. One of the reasons is that the lifetime of plasma blob could be small in the SOL of the LHD, because the connection length L_c dramatically drops away from the divertor leg. Thus, the bobby plasma transport has small effect on the density profile around the divertor legs in the LHD, compared with tokamaks. More quantitative evaluation of plasma blob transport should be required, such as velocity measurement of plasma blobs by using a reciprocating Langmuir probe with multi-electrodes[15].

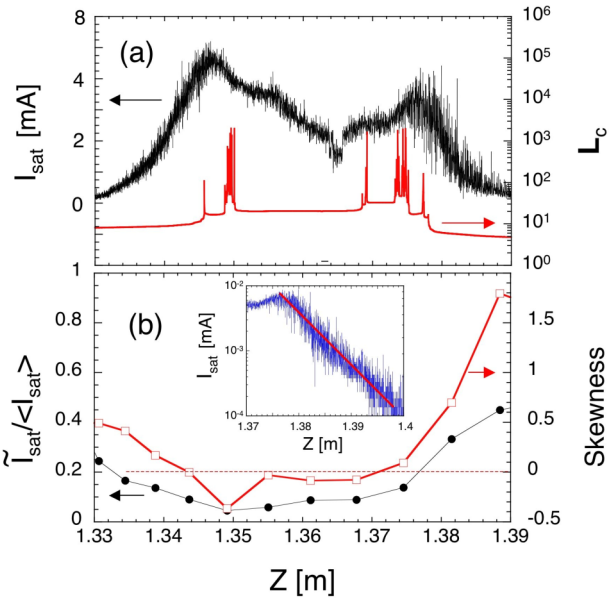

FIG. 9 (a) profile of I_{sat} around a plasma leg measured by the reciprocating Langmuir probe and magnetic connection length L_c, (b) profiles of normalized fluctuation amplitude and skewness of I_{sat} in Fig. 10(a). The inset shows logarithmic plot of I_{sat} at Z > 1.38 m.

4.2 Dependence of bursty fluctuation property on plasma parameters

In order to discuss the origin of the bursty fluctuation observed in this study, we will briefly mention what is a key parameter to determine the fluctuation property. We analyzed a set of I_{sat} date measured with the divertor probe array in a same magnetic configuration with different core plasma density. The statistical properties of these fluctuations show very weak core plasma density dependence. For a different magnetic axis operation of R_{rm} = 3.6 m, the same fluctuation properties of I_{is} are obtained at probe tips 5, 6, 7 shown in Fig. 1(b), because the magnetic configuration around probe electrodes 5,6,7 is quite similar to that around probe electrodes 9,10,11 for R_{rm} = 3.53 m. These experimental evidences indicate that the burst events are not determined by core plasma

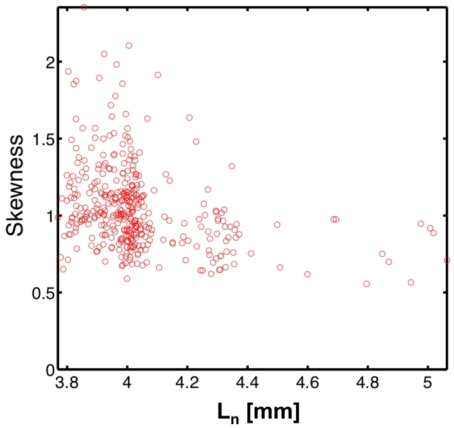

FIG. 10 Skewness of I_{sat} measured at probe 9 as a function of density decay length L_n.

density, and strongly influenced by the magnetic structure around the probe electrodes. Fig. 10 shows dependence of the skewness of I_{sat} data measured at probe 9 on the density decay length L_n. The length L_n is defined by

$$L_n^{-1} = \frac{2}{d_{9-10}} \cdot \frac{\left\langle I_{sat}^{10} \right\rangle - \left\langle I_{sat}^{9} \right\rangle}{\left\langle I_{sat}^{10} \right\rangle + \left\langle I_{sat}^{9} \right\rangle},$$

where $\left\langle I_{sat}^{9} \right\rangle$ and $\left\langle I_{sat}^{10} \right\rangle$ are time averaged value of the I_{sat} measured at probe 9 and 10, respectively. d_{9-10} is an interval between probe 9 and 10. Although the range of L_n is small, the skewness seems to be slightly increasing as decreasing L_n. But, at L_n below 4, the scattering of skewness values is quite large, which would suggest that the bursty fluctuation property can be determined not only by L_n but also other parameter.

5. Conclusion

We have investigated electrostatic fluctuation properties of I_{is} measured in the outboard divertor plate and in SOL region of the LHD. Bursty fluctuation characteristics is strongly influenced by the magnetic field structure around the probe electrodes Large positive burst events were observed in a lower magnetic field side of the divertor leg and the negative spikes was observed at striking point of the divertor leg. A reciprocating probe measurement also shows positive bursty events at a lower magnetic field side of the divertor leg. These experimental results agree with the theoretical prediction of plasma blob transport although the second SOL region with a flat density profile was not clearly observed. The bursty fluctuation was also analyzed to compare with the SOC modeling. Both shape of the power spectrum and waiting-time statistics give a disagreement with the SOC prediction.

Acknowledgments

We wish to thank Dr. Tsuji for fruitful discussion and comments, and also thank Mr. Takagi for his excellent technical supports. This work is supported by the NIFS budget NIFS03KLPP002 and NIFS04KZPD010. This work is also supported by NIFS/NINS under the project of Formation of International Network for Scientific Collaborations.

References

[1] ZWEBEM S.J., *et al., Nucl.Fusion* **23** (1983) 825.
[2] MOYER R.A., *et al., Plasma Phys. Control. Fusion* **38** (1996) 1273.
[3] BUDAEV V., *et al., Plasma Phys. Control. Fusion* **3** (1993) 429.
[4] ANTAR G.Y. *et al., Phys. Rev. Lett.* **87 (**2001) 065001.
[5] CARRERAS B.A. *et al., Phys. Plasmas* **8 (**2001) 3702.
[6] TERRY J.L. *et al., Phys. Plasmas* **10** (2003) 1739.
[7] KRASHENINNIKOV S., Phys. Lett. A **283**(2001) 368.
[8] BOEDO J. A. , *et. al.,* Phys. Plasmas, **10** (2003) 1670.
[9] MIYOSHI H., *et. al.* 31st EPS Plasma Physics Conference, London (2004) P5.101.
[10] MASUZAKI S. , *et. al.,* Nucl. Fusion, **42**, (2002) 750.
[11] BUDAEV V., *et. al.,* Nucl. Fusion, **46**, (2006) S181.
[12] DIAMOND P.H., *et. al.,* Phys. Plasma **2** (1995) 3640.
[13] POLIZER, P. A., *et. al.,* Phys. Rev. Lett. **84** (2000) 1192.
[14] SPADA E., *et. al.,* Phys. Rev. Lett. **86** (2001) 3032.
[15] OHNO N., *et. al.,* Contrib. Plasma Phys. **44** (2001) 222.